Journal of Power Sources 196 (2011) 9382–9390

Contents lists available at ScienceDirect

Journal of Power Sources

journal homepage: www.elsevier.com/locate/jpowsour

High performance polymer electrolytes based on main and side chain pyridine aromatic polyethers for high and medium temperature proton exchange membrane fuel cells

M. Georgezi[a,b], C.L. Chochos[b], N. Gourdoupi[b], S.G. Neophytides[b,c,*], J.K. Kallitsis[a,b,c,**]

[a] Department of Chemistry, University of Patras, GR-26500 Rio-Patras, Greece
[b] Advent Technologies SA, Patras Science Park, GR-26504 Rio-Patras, Greece
[c] Institute of Chemical Engineering and High Temperature Chemical Processes, ICE/HT-FORTH, P.O. Box 1414, GR-26504 Rio-Patras, Greece

ARTICLE INFO

Article history:
Received 4 February 2011
Received in revised form 12 April 2011
Accepted 7 June 2011
Available online 29 June 2011

Keywords:
Fuel cells
Polymeric materials
Structure–property relationships
Polymer electrolytes
Medium/high temperature PEM

ABSTRACT

Novel aromatic polyether type copolymers bearing side chain polar pyridine rings as well as combination of main and side chain pyridine units have been evaluated as potential polymer electrolytes for proton exchange membrane fuel cells (PEMFCs). The advanced chemical and physicochemical properties of these new polymers with their high oxidative stability, mechanical integrity and high glass transition temperatures (T_g's up to 270 °C) and decomposition temperatures (T_d's up to 480 °C) make them promising candidates for high and medium temperature proton exchange membranes in fuel cells. These copolymers exhibit adequate proton conductivities up to 0.08 S cm^{-1} even at moderate phosphoric acid doping levels. An optimized terpolymer chemical structure has been developed, which has been effectively tested as high temperature phosphoric acid imbibed polymer electrolyte. MEA prepared out of the novel terpolymer chemical structure is approaching state of the art fuel cell operating performance (135 mW cm^{-2} with electrical efficiency 45%) at high temperatures (150–180 °C) despite the low phosphoric acid content (<200 wt%) and the low platinum loading (ca. 0.7 mg cm^{-2}). Durability tests were performed affording stable performance for more than 1000 h.

1. Introduction

Fuel cells offer a reliable solution to the environmental friendly energy production since they have the flexibility to be adapted to the diverse energy sources. Among the different types of fuel cells, polymer electrolyte membrane fuel cells (PEMFCs) have the highest potential for market penetration addressing automotive and stationary applications [1]. Up to now, perfluorosulfonic ionomer membranes such as Nafion (Du Pont) and similar materials by other manufacturers [2–4] as well as alternative polymeric materials based on aromatic backbones [5–11] have been tested as polymer electrolyte membranes in fuel cells. According to the operation temperature, PEMFCs can be classified in three subcategories. The first category is based on the traditional low temperature PEMFCs with operation temperature up to 80 °C mainly due to their need for humidified gases since their high performance is closely related to the hydration level of the membrane.

Medium temperature PEMFCs are considered those with operation temperatures between 80 °C and 130 °C which are able to operate with low humidity gases [12–16]. This operation temperature range is the most preferable for automotive application and the working principle of medium temperature PEMFCs is based on the use of composite membranes operating under low humidity conditions or heterocycle based Brønsted bases that can act as anhydrous proton conductors. More specifically, heterocycles such as imidazole, pyrazole or benzimidazole have been demonstrated to be useful substitutes for water at temperatures up to 140 °C. Kreuer et al. emphasized the proton-conducting properties of nitrogen-containing aromatic heterocycles and discussed the relationship between structure, self-dissociation and proton conductivity. The pure materials exhibited moderate conductivities in the liquid state which was ascribed to some degree of self-dissociation and they are known for extraordinary thermal and/or chemical stability and have transport coefficients similar to those of water at higher temperatures. Similar to water, they are able to form hydrogen-bond networks, they are amphoteric and undergo autoprotolysis to a much higher degree than water leading to high proton conductivity even in the pure state. However, a general disadvantage of all

* Corresponding author at: Institute of Chemical Engineering and High Temperature Chemical Processes, ICE/HT-FORTH, P.O. Box 1414, GR-26504 Rio-Patras, Greece. Tel.: +30 2610 965265.
** Corresponding author at: Department of Chemistry, University of Patras, GR-26500 Rio-Patras, Greece. Tel.: +30 2610 962952; fax: +30 2610 997122.
E-mail addresses: neoph@iceht.forth.gr (S.G. Neophytides), j.kallitsis@upatras.gr (J.K. Kallitsis).

0378-7753/$ – see front matter © 2011 Elsevier B.V. All rights reserved.
doi:10.1016/j.jpowsour.2011.06.031

low molecular weight proton solvents is their volatility and hence, a high temperature application requires their immobilization in the polymer membrane where a high local mobility of the proton solvent and the protonic charge carriers therein has still to be guaranteed [17–23].

Finally, high temperature PEM fuel cells (140–200 °C) offer the distinct advantages of high carbon monoxide (CO) tolerance, enhanced kinetics on both electrodes, easier thermal management and the ability to use stack waste energy for heat cogeneration increasing the total efficiency and are the preferable choice for stationary applications. Polymeric materials of particular properties have to be used as electrolytes for high temperature MEAs in order to withstand the harsh conditions during the fuel cell operation. The polymeric material should possess good mechanical, thermal, chemical and oxidative stability, high glass transition temperature and high proton conductivity while the membrane electrode assembly (MEA) should possess good mechanical stability, long term chemical stability under continuous operation and cycling conditions and small voltage drop. Among the different ideas, the one that seems more mature and reliable is based on materials that combine acid–base interactions in order to acquire high proton conductivity (10^{-1} S cm^{-1}) at temperatures ranging between 140 °C and 200 °C.

Polybenzimidazole (PBI) [24–32] is the state of the art high temperature polymer electrolyte, combining high thermal stability with increased proton conductivity after doping with phosphoric acid. The polymeric membranes are imbibed with phosphoric acid so that the proton acceptor sites of the benzimidazole ring interact with the phosphoric acid molecules due to acid–base interactions providing conducting materials. Although PBI based systems have been extensively studied at various operating conditions, there are some drawbacks with regards to its moderate mechanical properties, specifically for the doped membranes with phosphoric acid, and low oxidative stability [30]. There is a significant research effort towards the development of some novel polymeric materials which can be used alternatively to PBI. One case is the simpler polybenzimidazole derivative poly(2,5-benzimidazole) (ABPBI) [33–36] that has been investigated as an alternative fuel cell membrane material. ABPBI doped with phosphoric acid provide membranes which are stable at the operating temperatures of high temperature PEM fuel cells.

Our approach towards the development of high temperature polymer electrolyte membranes is based on the use of aromatic polyether polymers or copolymers that bear pyridine units. Aromatic polyether backbones are chosen for their high mechanical, thermal and chemical stability, while the incorporation of polar pyridine groups aids in the retention of phosphoric acid [37–42]. In this paper, pyridine units are inserted in the polymer backbone either as side chain substituents or both as main chain units and side chain groups. The presence of side chain pyridine has enhanced the amount of absorbed phosphoric acid. Copolymers bearing sulfone, phosphinoxide and tetramethyl moieties have been prepared, combining different monomers that result in tailor made polymeric materials. All polymers are pre-screened in terms of their critical physicochemical properties and especially in relation to their phosphoric acid doping ability. Selected copolymers were fabricated into MEAs and their electrochemical features and fuel cell performance was studied at high temperatures.

2. Experimental

2.1. Instrumentation

Gel permeation chromatography (GPC) measurements were carried out using a Polymer Lab chromatographer equipped with two Ultra Styragel Columns (10^4, 500 Å), UV detector (254 nm), $CHCl_3$ as eluent and polystyrene standards for calibration. Dynamic mechanical analysis (DMA) measurements were carried out using a Solid-State Analyzer RSA II, Rheometrics Scientific Ltd., at 10 Hz. Thermogravimatric analysis (TGA) was carried out on 10 mg samples placed in alumina crucibles in a Labsys TM TG of Setaram under nitrogen and at a heating rate of 10 °C min^{-1}. Conductivity measurements were conducted by the four-probe current interruption method using a potentiostat/galvanostat (EG and G model 273) and an oscillator (Hitachi model V-650F). Electrochemical characterization including MEA conductivity and fuel cell performance testing was carried out using the potentiostat/galvanostat Autolab PGSTAT30 equipped with the Booster 20A (Eco Chemie).

2.2. Materials

Monomers and polymers were prepared according to literature procedure [43,44]. Bis(4-fluorophenyl)-sulfone, and 3,3′,5,5′-tetramethyl-[1,1′-biphenyl]-4,4′-diol were obtained from Aldrich. Solvents were purchased from Aldrich and were used without further purification.

For the materials used in electrode construction, carbon cloth supporting layer and catalyst powder (30 wt% Pt/Vulcan XC-72R) were purchased from E-TEK Inc., SAB carbon powder was purchased from Cabot Inc. and PTFE dispersion in water from Aldrich.

2.3. Membrane/electrodes preparation and MEA fabrication/characterization

The phosphoric acid content in the membrane (100–220 wt%) was controlled by immersing a dry membrane (dried at 160 °C for 3 d in order to remove any excess of dimethylacetamide after the casting procedure at 80 °C) in H_3PO_4 85 wt% at certain temperature and time depending on the sample's chemical structure. The electrodes were comprising carbon cloth from E-TEK Inc., and home made gas diffusion layer (GDL) and catalytic layer. The GDL was made of Shawinigan acetylene black (SAB) carbon powder and PTFE dispersion in water which was treated at 300 °C under static air for 40 min. The catalytic layer was prepared by spraying an ink on the GDL, which was prepared by mixing the catalyst powder (30 wt% Pt/C, E-TEK Inc.) and the desired amount of polymeric binder that was dissolved in DMA. The as prepared electrode was treated for 12 h at 80 °C and 3 d at 190 °C under vacuum in order to remove the organic solvent. Before the MEA assembly a certain amount of phosphoric acid was sprayed onto the catalytic layer.

The phosphoric acid impregnated membranes (doping level = 100 or 190 wt%) were sandwiched between the two Pt electrodes and were hot pressed at 150 °C for 5 min. In this work, the cathode side and the anode side use the same electrodes with catalyst loading 0.7–0.8 mg cm^{-2}.

Pure and dry hydrogen and oxygen gases were supplied to the anode and cathode compartments, respectively, for the operation of the cell at 120–180 °C and at ambient pressure. The effective dimensions of electrodes were 5 cm × 5 cm and the electrochemical evaluation was carried out in a single cell with serpentine flow channels (Fuel Cell Technologies Inc.). The measurements were made in two-electrode arrangement. Polarization curves were recorded at different temperatures using the potentiostat/galvanostat PGSTAT30 with the steady state current recorded for 30 s after each potential was set. The electrochemical impedance spectra (EIS) were recorded at 0.5 V and 0.65 V in the frequency range of 10 mHz to 20 kHz with an amplitude of sinusoidal signal of 10 mV, using the same equipment.

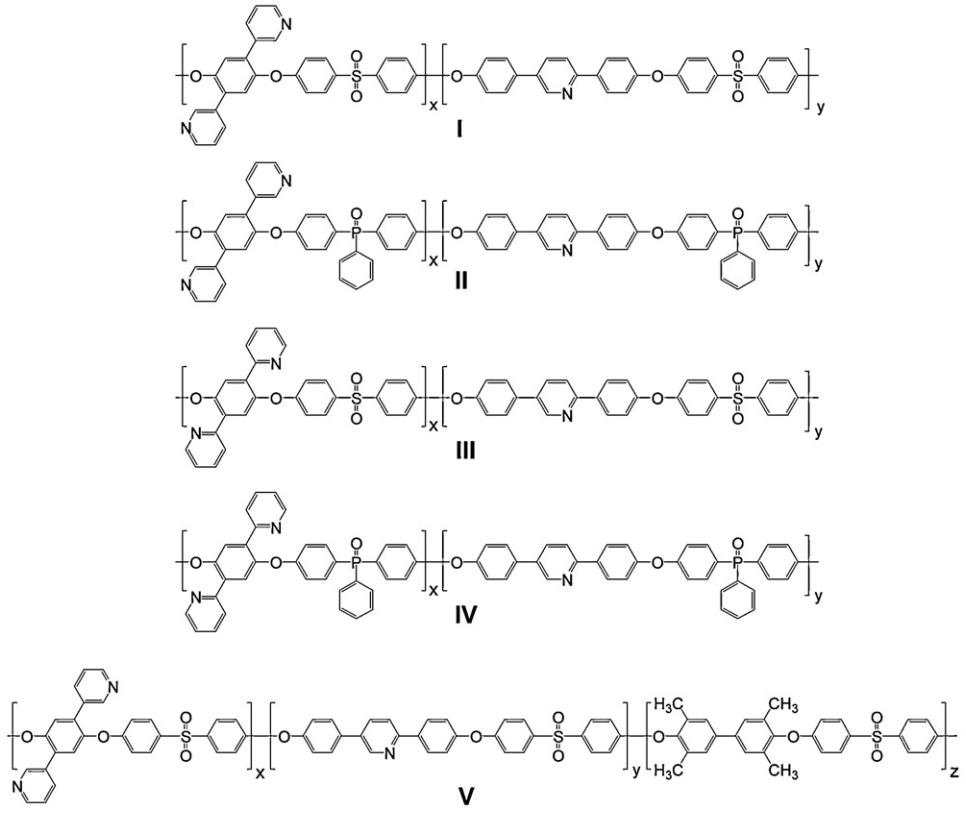

Scheme 1. Chemical structures of polymers **I–V**.

3. Results and discussion

3.1. Polymeric materials

In order to use heterocyclic groups, like pyridine, as possible interaction sites with the strong acids but at the same time considering those groups as solubilizing substituents of the rigid aromatic polymers, new monomers that possess the specific characteristic are needed. The diols 1,4-bis(2-pyridine)-hydroquinone and 1,4-bis(3-pyridine)-hydroquinone have been previously synthesized and used for aromatic polyether synthesis [43,44]. In this work these diols are used in combination with the linear 2,5-bis(4-hydroxyphenyl)-pyridine for the preparation of copolymers and terpolymers bearing side and main chain pyridine moieties. As it was shown previously the pyridine groups interact with the phosphoric acid molecules providing ionically conducting membranes based on aromatic polyethers [37–42]. The chemical structure of all the synthesized polymers are presented in Scheme 1.

In order to verify whether high molecular weights polymers with good film forming properties can be obtained by the use of the side pyridine diols, the copolymers 3-dPPy(*x*)coPES (**I**), 3-dPPy(*x*)coPO (**II**), 2-dPPy(*x*)coPES (**III**) and 2-dPPy(*x*)coPO (**IV**), where *x* is the percentage of the side pyridine diol, were synthesized. The molecular weights of **I–IV** which were measured using GPC are depicted in Table 1. Although interaction with the columns is possible, the copolymers **III** and **IV** demonstrate high molecular weights and in some cases good film forming properties were obtained (Table 1). The copolymers with the bis(4-fluorophenyl)-sulfone moiety exhibit better solubility when the content of the side pyridine diol is increased, while the opposite behaviour is observed in the case of the copolymers with the bis(4-fluorophenyl)-phenylphosphinoxide probably due to the different packing of the polymeric chains.

Table 1
Molecular weight characteristics of the synthesized copolymers **I–V**.

Code	Copolymers	M_n	M_w	PDI	Film quality
$\mathbf{I_a}$	3-dPPy(10)coPES	2000	2000	1.0	+
$\mathbf{I_b}$	3-dPPy(50)coPES	10,000	17,000	1.7	+++
$\mathbf{II_a}$	3-dPPy(10)coPO	16,000	31,000	1.9	+++
$\mathbf{II_b}$	3-dPPy(50)coPO	4000	6000	1.5	+
$\mathbf{III_a}$	2-dPPy(10)coPES	12,000	15,000	1.3	+
$\mathbf{III_b}$	2-dPPy(50)coPES	13,000	18,000	1.4	++
$\mathbf{IV_a}$	2-dPPy(10)coPO	15,000	25,000	1.7	++
$\mathbf{IV_b}$	2-dPPy(50)coPO	13,000	20,000	1.5	+
$\mathbf{V_a}$	3-dPPy(5)coPPy(57)T(38)S	52,000	75,000	1.4	+++

+, good; ++, very good; +++, excellent.

In an attempt to increase the solubility and as a sequence to further improve the film forming properties of the copolymers, the terpolymer 3-dPPy(5)coPPy(57)coT(38)S ($\mathbf{V_a}$, Scheme 1) has been synthesized and the chemical structure was verified by NMR spectroscopy. This copolymer is a modification of the general chemical structure of copolymer **I**, where the 3,3′,5,5′-tetramethyl-[1,1′-biphenyl]-4,4′-diol has been added, aiming to higher solubility at high molecular weights so that a membrane with good film forming properties can be achieved. The terpolymer $\mathbf{V_a}$ exhibit increased molecular weight as compared with all other copolymers examined here and excellent film forming properties (Table 1).

3.2. Mechanical properties and oxidative stability

Dynamic mechanical analysis (DMA) was used to examine the mechanical properties of the copolymers. The glass transition temperatures (T_g's) of the diphenylsulfone (3dPPy(*x*)coPES) and the phenylphosphinoxide (3dPPy(*x*)coPO) copolymers are in the range of 246–273 °C depending on the structure and the copolymer

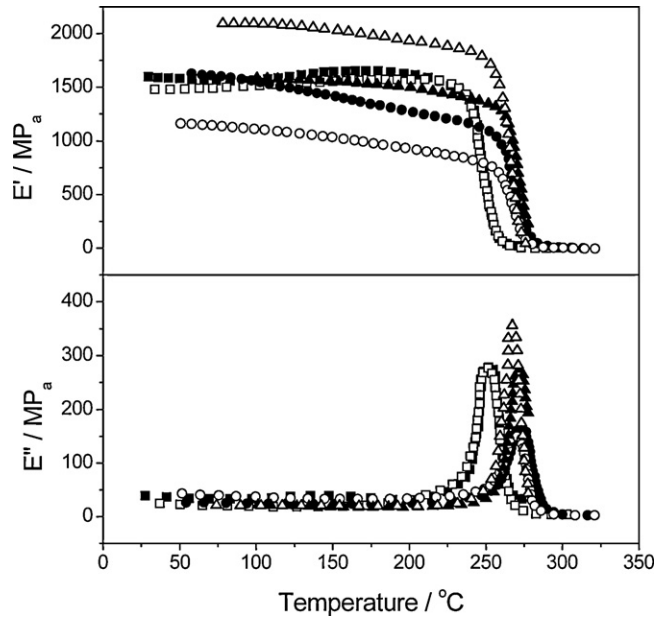

Fig. 1. Temperature dependence of the storage (E') and loss (E'') modulus for polymers: 3-dPPy(50)coPES (**I_b**), 3-dPPy(10)coPO (**II_a**) and 3-dPPy(5)coPPy(57)coT(38)S (**V_a**) before (■, ●, ▲) and after (□, ○, △) the treatment with H_2O_2, respectively.

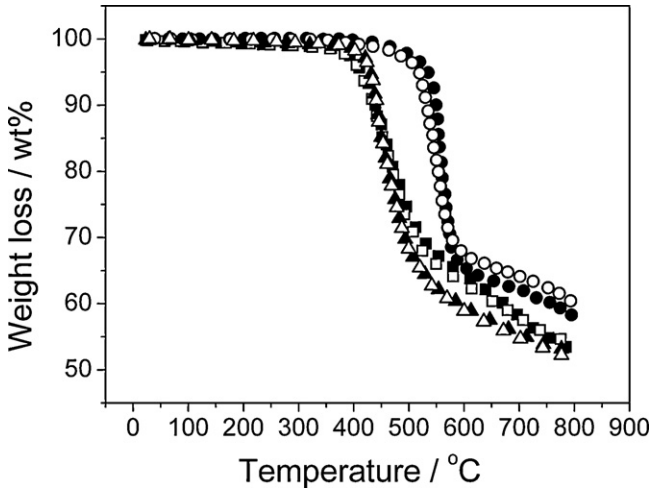

Fig. 2. Thermogravimetric analysis for polymers: 3-dPPy(50)coPES (**I_b**), 3-dPPy(10)coPO (**II_a**) and 3-dPPy(5)coPPy(57)coT(38)S (**V_a**) before (■, ●, ▲) and after (□, ○, △) the treatment with H_2O_2, respectively.

composition [44]. Comparing the same copolymer structures, an increase in the glass transition temperature was obtained as the percentage of the side pyridine diol in the copolymer decreases. The 2-pyridine substituted copolymers **III** and **IV** also exhibit high glass transition temperature in the range of 247–252 °C. The similar T_g values of all tested copolymers with similar M_W strongly indicate that the position of the nitrogen atom in the side pyridine ring does not influence the thermal transitions of the resulting materials.

Terpolymer **V_a** exhibits similar T_g value to the copolymers **I–IV**, thus indicating that the introduction of 3,3′,5,5′-tetramethyl-[1,1′-biphenyl]-4,4′-diol in the backbone of copolymer **I_b** did not affect the transition temperatures of the polymer. On the other hand, the introduction of the aforementioned diol leads to the synthesis of soluble polymers with high molecular weight (M_w > 70000), which is one of the main prerequisites for the casting of high quality membranes.

The chemical, thermal and oxidative stability of the copolymers was tested using the Fenton's test [45–47]. The membrane samples were immersed into 3 wt% H_2O_2 aqueous solution containing ferrous ions at 80 °C for 72 h. The weights of dried samples before and after the experiment were compared and found unchanged. In all cases, the membranes retained their mechanical integrity as measured with dynamic mechanical analysis (Fig. 1) and their high thermal stability (above 400 °C) as detected with thermogravimetric analysis (Fig. 2) before and after the treatment. Just for comparison, the polybenzimidazole (PBI) membranes are broken into small pieces (loss of mechanical integrity) after 30 min of exposure to the Fenton's test conditions, while after 20 h showed a weight loss of about 15% [30,47]. The reason for the superior oxidative stability of our materials is attributed to the more robust chemical structure of aromatic polyethers and the pyridine groups as compared to the more sensitive to oxidation imidazole rings in the PBI structure [48,49]. The argument whether the higher hydrophobicity of aromatic polyether polymer structures that have been synthesized in the present study, compared to PBI, protects the polymers from oxidation by preventing the penetration of the free radicals into the membrane's structure, was previously clarified by testing hydrophilic blends of our polymers with water soluble polymers, which were shown to withstand the oxidative degradation under identical Fenton's test conditions [50].

3.3. Doping ability

The doping ability of these film forming materials is of utmost importance since the ability of the polymeric membranes to absorb phosphoric acid determines to a certain extent the performance of the cell. The direct interactions of the phosphoric acid with either the pyridine or the imidazole moieties have been proven by means of FT-Raman spectroscopy [51]. These were shown by the blue shifts of the symmetric stretch of the imidazole group of the PBI and of the pyridine groups. The smaller blue shift of the symmetric stretch of the pyridine group with respect to the corresponding shift of the imidazole is in accordance with the weaker basic character of the pyridine group (imidazole pK_a: 7.0, pyridine pK_a: 5.25). These characteristic shifts were attributed to the positive charge that is being induced on the imidazole and pyridine groups due to the protonation of the corresponding nitrogen atoms by the phosphoric acid. These interactions though of ionic nature could not possibly contribute significantly to the ionic conductivity of the membrane

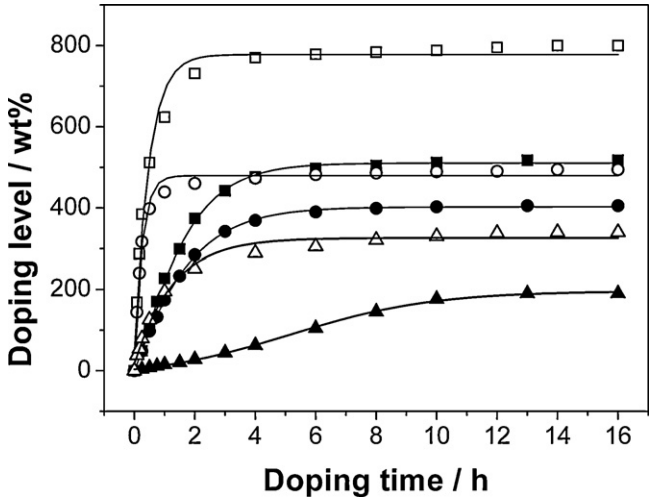

Fig. 3. Time dependence of doping level (wt%) of polymers: 3-dPPy(50)coPES (**I_b**), 3-dPPy(50)coPO (**II_b**) and 3-dPPy(10)coPO (**II_a**) at 25 °C (■, ●, ▲) and 50 °C (□, ○, △), respectively.

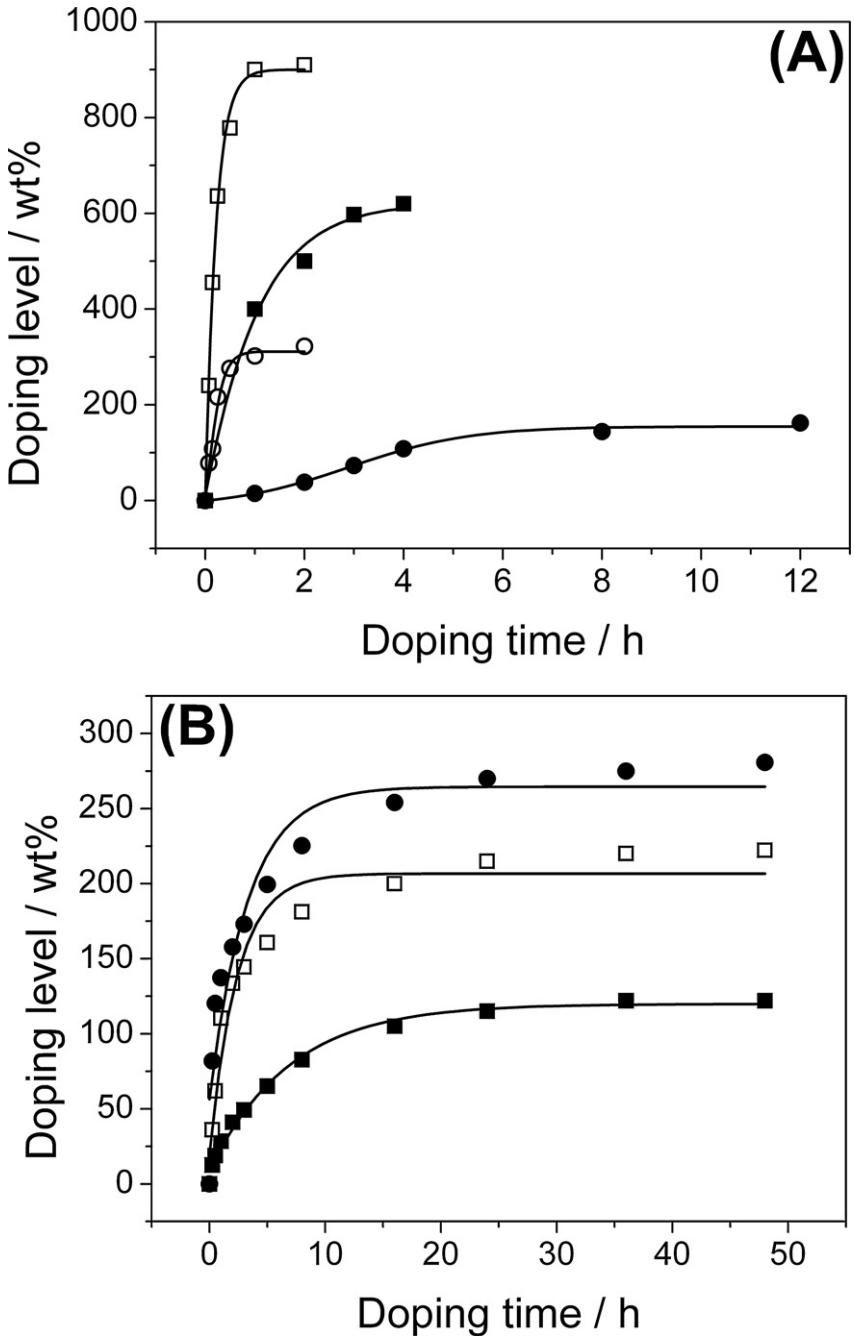

Fig. 4. Time dependence of doping level (wt%) of polymers: (a) 2-dPPy(50)coPES (**III$_b$**) and 2-dPPy(10)coPO (**IV$_a$**) at 25 °C (□, ●) and 50 °C (□ ,□) and (b) 3-dPPy(5)coPPy(57)coT(38)S (**V$_a$**) at 50 °C (■), 80 °C (□) and 100 °C (●), respectively.

due to their extent, as well as the size and the immobilization of the species involved. Instead they constitute the substrate on which the excess phosphoric acid network will be developed within the matrix of the polymer blend [52]. So, the conductivity depends not only on the basicity and the doping ability of the polymer electrolyte but also the structure of the polymer and the morphology play a significant role in the conduction mechanism.

The membranes were immersed into H_3PO_4 85 wt% at various temperatures and for different doping times. The evolution of the acid uptake of the membranes was followed by removing the imbibed membranes from the acid bath at successive time periods, wiped them dry and quickly weighted. The acid uptake of the membranes is defined as the weight percent (wt%) of the acid per 100 g of polymer. The doping level evolution with respect to time is depicted in Figs. 3 and 4. With increasing doping temperature and for higher side diol content, the phosphoric acid doping level increases, reaching plateau values at 800 wt% and 900 wt% H_3PO_4 doping level for the copolymers 3-dPPy(50)coPES (**I$_b$**) and 2-dPPy(50)coPES (**III$_b$**) respectively, at 50 °C and at relatively short period of time. It is worth mentioning that even at room temperature these copolymers exhibit extremely high doping ability reaching values as high as 500 wt%. More specifically, at 25 °C the copolymer 3-dPPy(50)coPES (**I$_b$**) reaches a value of about 500 wt% while copolymer 3-dPPy(50)coPO (**II$_b$**) reaches 400 wt%. At 50 °C doping values of 800 wt% and 500 wt% for copolymers 3-dPPy(50)coPES (**I$_b$**) and 3-dPPy(50)coPO (**II$_b$**) were obtained,

respectively. These measurements show in a systematic way that the copolymers with the sulfone groups achieve higher doping levels than the corresponding materials with phosphinoxide moieties. The present observation is opposed to our previous findings [39,40] where the presence of the phosphinoxide units improve the doping ability of the copolymers. This was attributed to the chain linearity interruption caused by the inserted phenylphosphinoxide units in the main polymeric backbone. These contradictory results show that the detailed polymeric structure is very crucial for the determination of the final behaviour of the polymeric membranes. In the present cases this differentiation can be attributed to the different packing of the polymeric chains due to the presence of the bulky side pyridine units. Thus, the interruption of the chain linearity caused by the introduction of the phenylphosphinoxide units in the main polymeric backbone, obtained in the previous studies [39,40,53], is probably balanced by the presence of the bulky substituents which may interrupt the chain linearity contributing also to the improved doping ability of these polymeric materials.

Comparison between the copolymers with the different position of the nitrogen atom of the side chain pyridine ring results with a controversial doping behaviour as shown in Fig. 4a. The copolymers with the bis(4-fluorophenyl)-sulfone moiety showed higher doping ability when the position of the nitrogen atom is at the 2 position (compare copolymer 2-dPPy(50)coPES (**III$_b$**) with 3-dPPy(50)coPES (**I$_b$**)), while the copolymers with the bis(4-fluorophenyl)-phenylphosphinoxide moieties exhibit higher doping ability when the position of the nitrogen atom is at the 3 position (compare copolymer 2-dPPy(10)coPO (**IV$_a$**) with 3-dPPy(10)coPO (**II$_a$**)).

Beyond the various differentiations in the doping ability of the aforementioned copolymers, which are related to variations in the chemical structure, the main conclusive remark is that the presence of the side diols in the polymer chemical structure affects significantly the doping ability of the polymeric membranes. This can be attributed to the different packing of the polymeric chains due to the presence of the bulky side pyridine units. Similar effect has been observed for the case of terpolymer 3-dPPy(5)coPPy(57)coT(38)S with only 5 mol% side pyridine diol (**V$_a$**), which approached high doping levels in the range of 300 wt% at 100 °C (Fig. 4b) retaining the good mechanical properties even at these high doping levels. The mechanical properties of the doped membranes have been tested. Doping of terpolymer with 200 wt% H_3PO_4 decreased the storage modulus due to intermolecular and intramolecular interactions that can alter the physical state of the polymer only two orders of magnitude giving values of 100 MPa in the temperature of 180 °C for the undoped terpolymer and 1 MPa in the temperature of 180 °C for the doped terpolymer, retaining thus the mechanical integrity of the terpolymer. As already mentioned it seems that the structure and most probably the different chain conformation and packing determine the doping behaviour. The effect of the side pyridine moiety is being proven if a comparison is made with the doping ability of the copolymer with similar chemical structure [38]. A 5 mol% insertion of the side pyridine diol in this structure resulted in an over 100 wt% increase in the H_3PO_4 doping level of the **V$_a$** copolymer, while maintaining the good membrane integrity.

3.4. Electrochemical characterization

Qualitative comparison of the mechanical integrity of the doped membranes, prepared by representative examples of each copolymer structure that are also good film formers, like copolymers 3-dPPy(50)coPES (**I$_b$**), 2-dPPy(50)coPES (**III$_b$**), 3-dPPy(10)coPO (**II$_a$**) and 2-dPPy(10)coPO (**IV$_a$**), was attempted. The copolymer **I$_b$** with the bis(4-fluorophenyl)-sulfone moiety and 50 mol% side pyridine (nitrogen in 3 position) diol and the terpolymer **V$_a$** with the three

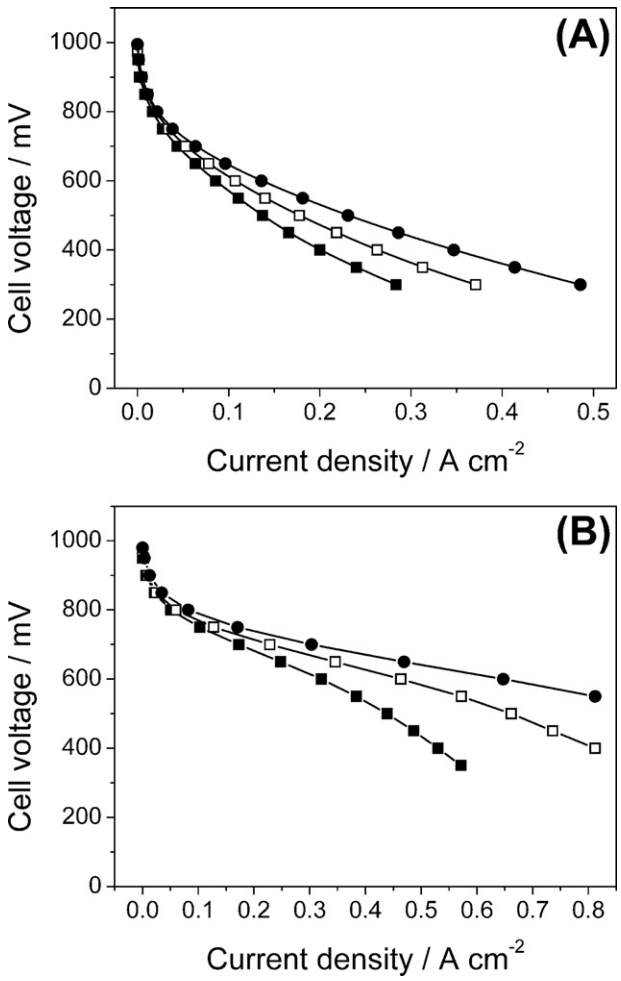

Fig. 5. Polarization curves for the copolymers: (a) 3-dPPy(50)coPES (**I$_b$**) at several temperatures between 120 °C (■), 130 °C (□), 140 °C (●) and (b) 3-dPPy(5)coPPy(57)coT(38)S (**V$_a$**) at 140 °C (■), 160 °C (□), 180 °C (●). Hydrogen: 1.2× stoichiometry, ambient pressure and 0% RH. Oxygen: 1.5× stoichiometry, ambient pressure and 0% RH.

structural units and 5 mol% side pyridine (nitrogen in 3 position) diol showed superior membrane integrity, after doping with H_3PO_4 85 wt% at 50 °C and 100 °C, respectively.

These copolymers were tested in a 25 cm^2 single cell. Though membrane integrity of the doped copolymer **I$_b$** is quite acceptable even at doping levels as high as 500 wt% at room temperature, the membrane was significantly plasticized and disrupted at elevated temperatures (>130 °C). In order to avoid the plasticization effect at high temperatures, MEAs based on copolymer **I$_b$** with doping level as low as 100 wt% were prepared. The thickness of the membrane after doping with H_3PO_4 is 170 μm. The Pt loading of the electrodes was 0.7 mg cm^{-2} and they were doped with 8 g H_3PO_4 per 1 g of Pt in order to achieve good electrochemical interface with high aspect ratio so that the electrochemical reaction rate is maximised. Similar MEA using the same electrodes was also prepared using terpolymer **V$_a$** with doping level 190 wt% and thickness 80 μm. Fig. 5 illustrates the polarization curves of the fuel cells at several operating temperatures ranging between 120 and 140 °C (Fig. 5a MEA with **I$_b$**) and 140–180 °C (Fig. 5b MEA with **V$_a$**), using dry gases of hydrogen and oxygen with anode and cathode inlet molar flow rates 180 cm^3 min^{-1} and 113 cm^3 min^{-1}, for H_2 and O_2 respectively, at ambient pressure. As expected the MEAs' performance is improved for both cells with increasing temperature.

The MEA based on **I$_b$** copolymer is inferior to the terpolymer **V$_a$** MEA both in terms of performance and its ability to operate

at higher temperature. Its lower performance in comparison to the performance of terpolymer **V_a** at 140 °C is due to the thicker membrane used (copolymer **I_b**). In addition the inability of the **I_b** MEA to operate at temperatures above 140 °C is attributed to problems related to the membrane integrity due to severe plasticization caused by the phosphoric acid at elevated temperatures. On the contrary the MEA based on **V_a** terpolymer performs in a very satisfactory way even at 180 °C. Its current–voltage performance with H_2 and O_2 at ambient pressure and 180 °C (650 mA cm^{-2} at 0.6 V) or 160 °C (460 mA cm^{-2} at 0.6 V) is depicted in Fig. 5b. The *IV* curve of the MEA based on **V_a** terpolymer compares well with the performance of state of the art MEAs based on PBI [30], at 160 °C under H_2/air, which is among the highest in the open literature. Just for comparison, the *IV* curves of the MEAs based on **V_a** terpolymer at 180 °C under H_2/air and PBI at 160 °C under H_2/air give comparable results [30].

The MEAs' ionic and polarization resistances were measured by means of AC impedance. The spectra recorded for both **I_b** and **V_a** MEAs are depicted as Nyquist plots on a complex plane in Fig. 6 at different temperatures during fuel cell operation at 0.5 V and 0.65 V, respectively. The AC spectra under polarization conditions were recorded within the range of 50 kHz to 10 mHz in order to get reliable values of the ionic resistance and conductivity under operating conditions.

It is well known from the literature that the conductivity of the H_3PO_4 imbibed polymer electrolytes depends on the partial pressure of water [28], which under fuel cell operating conditions is produced at the cathode [51,52]. The effect of the partial pressure of water on the proton conductivity of the membrane is significant up to 5 kPa. Thereafter according to reference [52] the conductivity of the membrane does not vary significantly. Therefore a negligible variation is expected at varying current densities obtained at cell voltage of 0.5 V. The high frequency intersection with the real axis corresponds directly to the ionic resistance of the MEA. Note that the contact resistances of the MEA and the current collectors were negligible compared to the ionic resistance of the MEA. The distance between the high and low frequency intersection with the real axis corresponds to the polarization resistance of the electrochemical interfaces at the anode and cathode. In general the Nyquist plots of Fig. 6 can be simulated by two semicycles which rather correspond to the anodic (high frequencies arc) and cathodic (low frequencies arc) electrocatalytic processes (Table 2) [54]. The anodic H_2 oxidation reaction being faster than the cathodic O_2 reduction reaction appears at higher frequencies and with lower polarization resistance. As shown in Table 2 the two arcs were simulated with constant phase elements. The equivalent circuit is shown in the inset of Fig. 6.

Both ionic and polarization resistances decrease with increasing temperature. As already mentioned the ionic resistance of the **I_b** copolymer is higher than that of terpolymer **V_a** due to the twice as thick membrane. However as shown in Fig. 7a the ionic conductivity values, in the range of 0.03–0.08 S cm^{-1}, derived from the spectra of Fig. 6 are similar for both MEAs with similar activation energies 17.9 kJ mol^{-1} and 20.1 kJ mol^{-1}, respectively. These

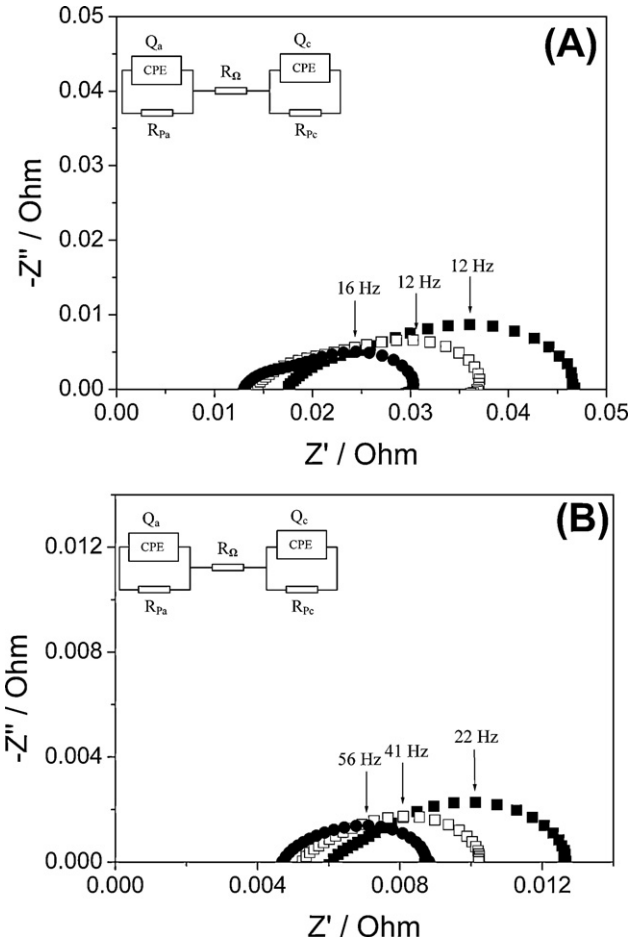

Fig. 6. Nyquist plot for the copolymers: (a) 3-dPPy(50)coPES (**I_b**) as a function of temperature at 120 °C (■), 130 °C (□), 140 °C (●) and (b) 3-dPPy(5)coPPy(57)coT(38)S (**V_a**) at 140 °C (■), 160 °C (□), 180 °C (●). FH_2: 1 l min^{-1}, ambient pressure and 0% RH. FO_2: 1 l min^{-1}, ambient pressure and 0% RH.

are typical values for H_3PO_4 imbibed membranes [52]. It is worth noticing that copolymer **I_b** though at lower doping level (100 wt%) exhibits similar proton conductivities at the same temperatures to the corresponding proton conductivities of terpolymer **V_a** being at higher doping level (190 wt%). This observation consolidates the conclusion that the polymer matrix plays significant role in proton conductivity of the H_3PO_4 imbibed membranes [51,52]. This, in combination to the proven interaction of steam with the H_3PO_4/polymer matrix, are considered as the main factors that determine the proton conductivity through the phosphoric acid imbibed polymer electrolytes. As has been recently reported, the hydration enthalpy of the phosphoric acid imbibed polymers varies upon varying the polymer matrix [52]. According to the aforementioned results, the hydration enthalpy of the H_3PO_4/polymer matrix is by a factor of two higher than the hydration enthalpy

Table 2
The ionic resistance of the electrolyte R_{el} and the polarization resistances R_1 and R_2 based on the fitting of the Niquist plots of Fig. 6.

	T (°C)	R_{el} (Ω)	$R_{p,A}$ (Ω)	$Y_{0,A}$ (S s$^{0.5}$ cm^{-2})	n_A	$R_{p,C}$ (Ω)	$Y_{0,C}$ (S s$^{0.5}$ cm^{-2})	n_C	ω_{max} (Hz)	
									Anode	Cathode
MEA **I_b**	120	0.017	0.012	0.68	0.7	0.017	1.15	0.936	142	12
	130	0.014	0.010	0.433	0.76	0.013	1.33	0.93	142	12
	140	0.013	0.007	0.39	0.78	0.011	1.31	0.93	359	16
MEA **V_a**	140	0.006	0.002	2.87	0.7	0.005	2.24	0.936	489	22
	160	0.005	0.001	2.15	0.76	0.004	2.16	0.9	906	41
	180	0.005	0.001	1.7	0.86	0.003	2.09	0.84	1233	56

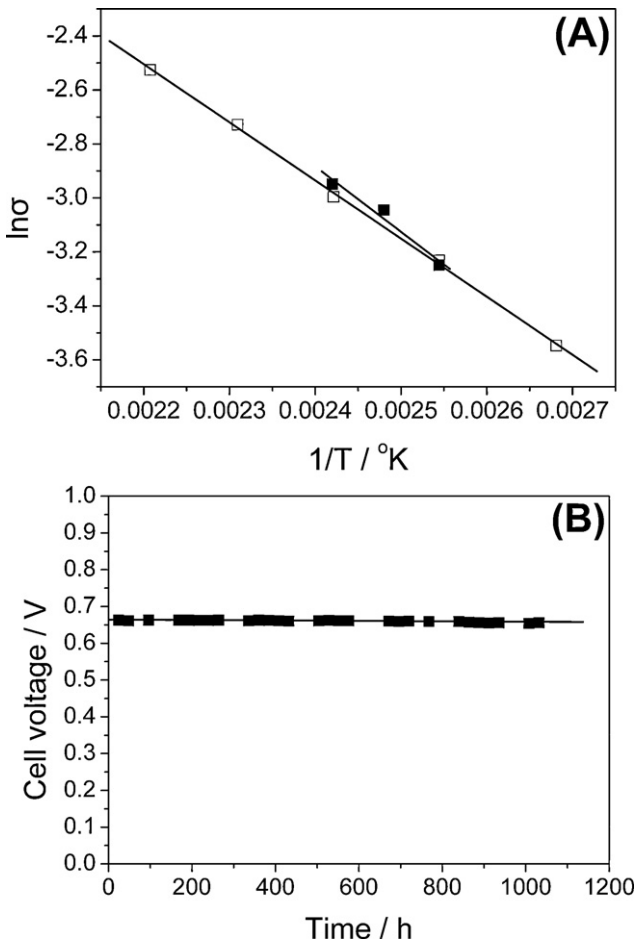

Fig. 7. (a) Effect of temperature on MEAs conductivity under fuel cell operating conditions for the copolymer 3-dPPy(50)coPES (**I$_b$**) at cell voltage 0.5 V (■) and 3-dPPy(5)coPPy(57)coT(38)S (**V$_a$**) at cell voltage 0.65 V (□), respectively. The data were derived from the AC impedance spectra of Fig. 6. (b) Long term stability test of the MEA prepared with terpolymer **V$_a$** at cell current density 0.2 A cm^{-2} using H_2 and air dry gases and stoichiometries 1.2 and 2 respectively. Operating temperature 180 °C.

of pure H_3PO_4. This interaction has been considered as of vital importance for the efficient facilitation of the Grotthus proton conduction mechanism taking into consideration that water molecules can play the role of proton carrier. Thus according to the Grotthus proton conduction mechanism protons are hopping either between aligned hydronium and water molecules or between water and H_3PO_4.

The performance of the MEA based on terpolymer **V$_a$** is very impressive. By tuning its chemical structure, it was possible to prepare H_3PO_4 imbibed membranes with very good membrane integrity and high doping level showing good ionic conductivities (0.08 S cm^{-1} at 180 °C) under fuel cell operation. This was accomplished by controlling the content of the side pyridine diol so as to tune the doping level of the membrane in H_3PO_4 and the content of 3,3′,5,5′-tetramethyl-[1,1′-biphenyl]-4,4′-diol which provided the good mechanical integrity. It must be noted that the aforementioned high proton conductivity and fuel cell performance has been achieved with the lowest doping level known in the open literature.

The stable performance of the MEA based on terpolymer **V$_a$** is depicted in the long term stability test in Fig. 7b, which was conducted at 0.2 A cm^{-2} and 180 °C for ca. 1000 h. The MEA impressively shows very small degradation 5 μV h^{-1}, thus being rendered as highly promising state of the art MEA for real high temperature PEM fuel cell applications.

4. Conclusions

The main scope of this work was the detailed characterization of new polymeric electrolytes bearing side chain and main chain pyridine units and their evaluation as potential membranes for use in medium and high temperature PEM fuel cells. The rigid aromatic character of these polymeric backbones results in good mechanical properties and excellent thermal and oxidative stability, while the introduction of the pyridine moieties provided more active sites for bonding of the phosphoric acid molecules demonstrating very high and controllable acid uptake of the polymers. The doping ability of these copolymers can be adjusted and the maximum obtained values are comparable with those of PBI even at room temperature showing the strong interaction tendency. The conductivity values of the polymers are well above the 10^{-2} S cm^{-1} even for low doping levels. Through the study of the various chemical structures in combination with membranes properties, an optimized chemical structure based on the terpolymer (**V$_a$**) has been successfully developed which posses all the specifications for an effective high temperature polymer electrolyte, providing finally technically useful membranes. Preliminary fuel cell tests at temperatures up to 180 °C using dry gases and low Pt loading at the electrodes were made. The performance and stability of the terpolymer **V$_a$** MEA is very impressive, despite the relatively low phosphoric acid doping level and can be considered among the state of the art materials and MEAs for high temperature PEM fuel cell applications.

Acknowledgements

Financial support of this work from the European Commission through the programs Energy K5-CT-2001-00572 (2001–2004) and NMP3 CT-2006-033228 (2006–2009) is greatly acknowledged.

References

[1] B.C.H. Steele, A. Heinzel, Nature 414 (2001) 345–352.
[2] K.A. Mauritz, R.B. Moore, Chem. Rev. 104 (2004) 4535–4586.
[3] M. Rikukawa, K. Sanui, Prog. Polym. Sci. 25 (2000) 1463–1502.
[4] R. Borup, J. Meyers, B. Pivovar, Y.S. Kim, R. Mukundan, N. Garland, D. Myers, M. Wilson, F. Garzon, D. Wood, P. Zelenay, K. More, K. Stroh, T. Zawodzinski, J. Boncella, J.E. McGrath, M. Inaba, K. Miyatake, M. Hori, K. Ota, Z. Ogumi, S. Miyata, A. Nishikata, Z. Siroma, Y. Uchimoto, K. Yasuda, K.-I. Kimijima, N. Iwashita, Chem. Rev. 107 (2007) 3904–3951.
[5] M.A. Hickner, H. Ghassemi, Y.S. Kim, B.R. Einsla, J.E. McGrath, Chem. Rev. 104 (2004) 4587–4612.
[6] B. Smitha, S. Sridhar, A.A. Khan, J. Membr. Sci. 259 (2005) 10–26.
[7] J.A. Kerres, J. Membr. Sci. 185 (2001) 3–27.
[8] J. Kerres, F. Schonberger, A. Chromik, T. Haring, L. Qingfeng, J.O. Jensen, C. Pan, P. Noye, N.J. Bjerrum, Fuel Cells 8 (2008) 175–187.
[9] J. Roziere, D.J. Jones, Annu. Rev. Mater. Res. 33 (2003) 503–555.
[10] L. Qingfeng, R. He, J.O. Jensen, N.J. Bjerrum, Chem. Mater. 15 (2003) 4896–4915.
[11] J. Zhang, Z. Xie, J. Zhang, Y. Tang, C. Song, T. Navessin, Z. Shi, D. Song, H. Wang, D.P. Wilkinson, Z.-S. Liu, S. Holdcroft, J. Power Sources 160 (2006) 872–891.
[12] P.L. Antonucci, A.S. Arico, P. Creti, E. Ramunni, V. Antonucci, Solid State Ionics 125 (1999) 431–437.
[13] G. Alberti, M. Casciola, Annu. Rev. Mater. Res. 33 (2003) 129–154.
[14] G. Alberti, M. Casciola, M. Pica, T. Tarpanelli, M. Sganappa, Fuel Cells 5 (2005) 366–374.
[15] L. Gatto, A. Sacca, A. Carbone, R. Pedicini, E. Passalacqua, J. Fuel Cell Sci. Technol. 3 (2006) 361–365.
[16] A.S. Arico, V. Baglio, A. Di Blasi, P. Creti, P.L. Antonucci, V. Antonucci, Solid State Ionics 161 (2003) 251–265.
[17] K.-D. Kreuer, S.J. Paddison, E. Spohr, M. Schuster, Chem. Rev. 104 (2004) 4637–4678.
[18] K.-D. Kreuer, Chem. Mater. 8 (1996) 610–641.
[19] M.F.H. Schuster, W.H. Meyer, M. Schuster, K.D. Kreuer, Chem. Mater. 16 (2004) 329–337.
[20] G. Scharfenberger, W.H. Meyer, G. Wegner, M. Shuster, K.-D. Kreuer, J. Maier, Fuel Cells 6 (2006) 237–250.
[21] Md.A.B.H. Susan, A. Noda, S. Mitsushima, M. Watanabe, Chem. Commun. 8 (2003) 938–939.
[22] M.F.H. Schuster, W.H. Meyer, Annu. Rev. Mater. Res. 33 (2003) 233–261.
[23] K.-D. Kreuer, J.T. Hynes, J.P. Klinman, H.H. Limbach, R.L. Schowen, Proton Conduction in Fuel Cells in Hydrogen-Transfer Reactions, Wiley-VCH, 2007.

[24] J.S. Wainright, J.T. Wang, D. Weng, R.F. Savinell, M.H. Litt, J. Electrochem. Soc. 142 (1995) L1121.
[25] J.-T. Wang, R.F. Savinell, J.-S. Wainright, M. Litt, H. Yu, Electrochim. Acta 41 (1996) 193–197.
[26] R. Bouchet, E. Siebert, Solid State Ionics 118 (1999) 287–299.
[27] V. Deimede, G. Voyiatzis, J.K. Kallitsis, L. Qingfeng, N.J. Bjerrum, Macromolecules 33 (2000) 7609–7617.
[28] Y.L. Ma, J.S. Wainright, M.H. Litt, R.F. Savinell, J. Electrochem. Soc. 151 (2004) A8–A16.
[29] J.A. Kerres, Fuel Cells 5 (2005) 230–247.
[30] L. Qingfeng, J.O. Jensen, R.F. Savinell, N.J. Bjerrum, Prog. Polym. Sci. 34 (2009) 449–477.
[31] A. Carollo, E. Quartarone, C. Tomasi, P. Mustarelli, F. Belotti, A. Magistris, F. Maestroni, M. Parachini, L. Garlaschelli, P.P. Righetti, J. Power Sources 160 (2006) 175–180.
[32] L. Xiao, H. Zhang, T. Jana, E. Scanlon, R. Chen, E.-W. Choe, L.S. Ramanathan, S. Yu, B.C. Benicewicz, Fuel Cells 5 (2005) 287–295.
[33] J.A. Asensio, P. Gomez-Romero, Fuel Cells 5 (2005) 336–343.
[34] J.A. Asensio, S. Borros, P. Gomez-Romero, J. Membr. Sci. 241 (2004) 89–93.
[35] H.J. Kim, S.Y. Cho, S.J. An, Y.C. Eun, J.Y. Kim, H.K. Yoon, H.J. Kweon, K.H. Yew, Macromol. Rapid Commun. 25 (2004) 894–897.
[36] J.A. Asensio, S. Borro, P. Gomez-Romero, J. Polym. Sci. Part A: Polym. Chem. 40 (2002) 3703–3710.
[37] N. Gourdoupi, A.K. Andreopoulou, V. Deimede, J.K. Kallitsis, Chem. Mater. 15 (2003) 5044–5050.
[38] E.K. Pefkianakis, V. Deimede, M.K. Daletou, N. Gourdoupi, J.K. Kallitsis, Macromol. Rapid Commun. 26 (2005) 1724–1728.
[39] N. Gourdoupi, K. Papadimitriou, S. Neophytides, J.K. Kallitsis, Fuel Cells 8 (2008) 200–208.
[40] M. Geormezi, V. Deimede, N. Gourdoupi, N. Triantafyllopoulos, S. Neophytides, J.K. Kallitsis, Macromolecules 41 (2008) 9051–9056.
[41] M.K. Daletou, N. Gourdoupi, J.K. Kallitsis, J. Membr. Sci. 252 (2005) 115–122.
[42] N. Gourdoupi, J.K. Kallitsis, S. Neophytides, J. Power Sources 195 (2010) 170–174.
[43] M. Geormezi, PhD Thesis, University of Patras, Greece, 2009.
[44] M. Geormezi, N. Gourdoupi, US Patent 7,786,244 (2010).
[45] A. Panchenko, A. Dilger, E. Moller, T. Sixt, E. Roduner, J. Power Sources 127 (2004) 325–330.
[46] G. Hubner, E. Roduner, J. Mater. Chem. 9 (1999) 409–418.
[47] Q. Li, C. Pan, J.O. Jensen, N.J. Bjerrum, Chem. Mater. 19 (2007) 350–352.
[48] R.A. Gaudiana, R.T. Conley, J. Polym. Sci. 7B (1969) 793–801.
[49] Z. Chang, H. Pu, D. Wan, L. Liu, J. Yuan, Z. Yang, Polym. Degrad. Stab. 94 (2009) 1206–1212.
[50] J.K. Kallitsis, M. Geormezi, S. Neophytides, Polym. Int. 58 (2009) 1226–1233.
[51] M.K. Daletou, J.K. Kallitsis, G. Voyiatzis, S.G. Neophytides, J. Membr. Sci. 326 (2009) 76–83.
[52] J. Kallitsis, in: C. Vayenas, R.E. White (Eds.), Modern Aspects of Electrochemistry, Springer, NY, 2011.
[53] M.K. Daletou, M. Geormezi, E.K. Pefkianakis, C. Morfopoulou, J.K. Kallitsis, Fuel Cells 10 (2010) 35–44.
[54] J.L. Jespersen, E. Schaltz, S.K. Kaer, J. Power Sources 191 (2009) 289–296.